Reconstruction of optical wavefronts with parallel registration algorithms

Nikolaus Berlakovich*[1], Martin Fuerst[1], Ernst Csencsics[1], and Georg Schitter[1]

[1]Christian Doppler Laboratory for Precision Engineering for Automated In-Line Metrology,
Automation and Control Institute (ACIN), TU Wien,
1040 Vienna, Austria

ABSTRACT

This paper presents an evaluation of three developed parallel registration algorithms for the reconstruction of optical wavefronts. Two practical use cases are considered including high-quality optics generating (i) a plane and (ii) a divergent wavefront. The wavefronts are measured segment-by-segment with a scanning Shack-Hartmann sensor measurement system and are reconstructed by the algorithms. As a benchmark for the comparison of the registration performance, the well-established iterative closest point (ICP) algorithm is used. Results show that the developed registration algorithms attain a registration precision up to a factor of 10 better than the registration precision of the ICP algorithm.

Keywords: Algorithms; Optical Metrology; Wavefronts; Testing

1. INTRODUCTION

Wavefront sensors[1] enable the evaluation of optical systems, as its performance is directly related to the transformation of a wavefront that is entering the system. The complete measurement of a wavefront is not possible if the wavefront exceeds the aperture size of the wavefront sensor or its dynamic range. More sophisticated measurement systems have to be used to measure these wavefronts, e.g. a wavefront sensor in combination with null optics[2] or a wavefront sensor in combination with a positioning system.[3,4] The latter one offers advantages, such as a higher flexibility with respect to the shape of the wavefront and no additional aberrations due to null-optics. Using a positioning system with 5 degrees of freedom (DOF), an almost arbitrarily shaped wavefront can be scanned with the wavefront sensor. During the scan, segments of the wavefront are measured at different locations. The entire wavefront is then reconstructed by registering the segments using the positioning data of the sensor. Due to uncertainties in the positioning system, registration algorithms are of great importance to obtain a high-quality reconstruction of the wavefront. Recently, three registration algorithms have been proposed, i.e. a parallel registration (PR),[5] a fast parallel registration (FPR)[6] and an iterative fast parallel registration (IFPR)[7] algorithm, where the segments of a wavefront are registered in parallel to attain small registration errors. In the individual publications the performance and functionality of the registration algorithms are evaluated and proven in the scope of a simulation-based analysis.

The contribution of this paper is the experimental evaluation and comparison of the PR, the FPR and the IFPR algorithm based on two use cases, i.e. the reconstruction of a plane and a divergent wavefront generated by real optical systems. In addition to the parallel registration algorithms, the well-established iterative closest point (ICP)[8] algorithm is considered as a benchmark. Section 2 introduces the measurement concept and the registration algorithms. Section 3 presents and discusses the experimental results and Section 4 concludes the paper.

Further author information: (Send correspondence to Nikolaus Berlakovich)
Nikolaus Berlakovich: E-mail: berlakovich@acin.tuwien.ac.at, Telephone: +43 (0) 1 58801 376 529

Pre-Print version of the article: Nikolaus Berlakovich, Martin Fuerst, Ernst Csencsics, and Georg Schitter, "Reconstruction of optical wavefronts with parallel registration algorithms," *SPIE Optics + Photonics 2022* Vol. 12221, pp. 192–198, 2022. DOI: 10.1117/12.2632961

2. MEASUREMENT CONCEPT AND REGISTRATION ALGORITHMS

The used measurement system is illustrated in Fig. 1 where a Shack-Hartmann sensor (HR-2, Optocraft, Erlangen, Germany) is mounted on a multi-axis positioning system (MAPS). The MAPS with 5 DOF is composed of three linear stages (VT-80, PI Physik Instrumente, Braunschweig, Germany) and two rotational stages (RM-3, Newmark Systems Inc., California) enabling scanning of complex shaped wavefronts with a diameter of up to $100\,mm$.[4] The Shack-Hartmann sensor (SHS) is a frequently used wavefront sensor, providing a reference free measurement that is insensitive to vibrations.[9] The optical system under test generates a wavefront which is then scanned by the measurement system, where the SHS measures the wavefront at multiple locations. In each SHS-measurement a specific segment of the wavefront is measured. In particular, the gradient of the wavefront segment is measured at points of a grid defined by the lenslet array in the aperture of the SHS[10] where each lenslet corresponds to a grid point. The wavefront segment is then reconstructed from the gradients using zonal reconstruction algorithms.[11] Using the positioning data of the MAPS for each SHS-measurement, registration of the wavefront segments is carried out to reconstruct the entire wavefront. For partially overlapping wavefront segments an overlap mismatch between the segments is observed, reflecting registration errors caused by uncertainties in the MAPS. The desired registration can be obtained by minimizing the overlap mismatch between the segments using registration algorithms. The registration algorithm determines the transformation of the segments for which the overlap mismatch has its global minimum. The transformation consists of a translation, a rotation and a wavefront propagation of each segment. The translation and the rotation are with respect to the three spatial dimensions. The wavefront propagation corresponds to the propagation of the segment along its surface normals.

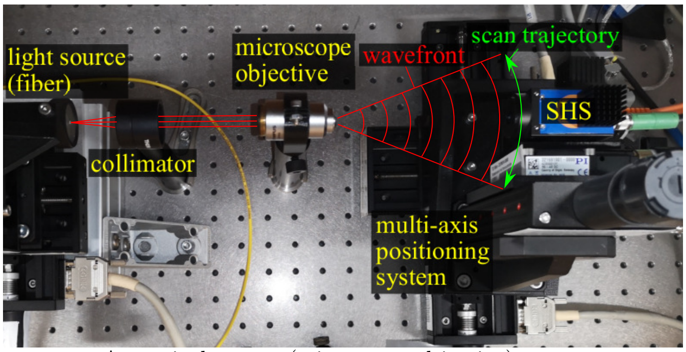

Figure 1: Measurement system. An optical system (microscope objective) generates a wavefront which is scanned by the SHS mounted on a MAPS. During scanning, the SHS measures segments of the wavefront.

From the reconstruction of a segment from an SHS-measurement a point cloud is determined representing the segment. The positioning data of the MAPS during the SHS-measurement is used to transform the point cloud from the local coordinate system of the sensor into the global frame (FG), leading to a coarse registration of the segments due to uncertainties in the MAPS (see Fig. 2a). The transformation consists of a translation denoted by $\boldsymbol{T}_{0i} \in \mathbb{R}^3$, a rotation denoted by a rotation-matrix $\boldsymbol{R}_{0i} \in \mathbb{R}^{3\times 3}$ and a wavefront propagation denoted by $S_{0i} \in \mathbb{R}$ where the lower index i is referring to a certain segment. Usually, S_{0i} equals 0, if ideal scanning of the wavefront is assumed where no phase differences between the segments are observed. Starting from the configuration of the segments based on $\boldsymbol{T}_{0i}$, $\boldsymbol{R}_{0i}$ and S_{0i}, the segments are then translated, rotated and propagated for the fine registration (see Fig. 2b) defined by the parameters $\boldsymbol{k}_i^* \in \mathbb{R}^3$, $\boldsymbol{\theta}_i^* \in \mathbb{R}^3$ and $s_i^* \in \mathbb{R}$, respectively, where s_i^* is equal to the distance of propagation. For reasons of clarity, the parameters of a segment are collected in the vector $\boldsymbol{a}_i^{*T} = (\boldsymbol{k}_i^{*T}, \boldsymbol{\theta}_i^{*T}, s_i^*) \in \mathbb{R}^7$ and the parameters of all segments are collected in $\boldsymbol{A}^{*T} = (.\, \boldsymbol{a}_i^{*T}\, .) \in \mathbb{R}^{7\,U}$, where U is equal to the total number of segments.
To determine the transformation for fine registration, a metric corresponding to the global overlap mismatch between the segments is minimized with respect to the transformation parameters $\boldsymbol{A}$. The global overlap mismatch is considered to obtain parallel registration of the segments and the corresponding metric is given by the

Pre-Print version of the article: Nikolaus Berlakovich, Martin Fuerst, Ernst Csencsics, and Georg Schitter, “Reconstruction of optical wavefronts with parallel registration algorithms,” *SPIE Optics + Photonics 2022* Vol. 12221, pp. 192–198, 2022.
DOI: 10.1117/12.2632961

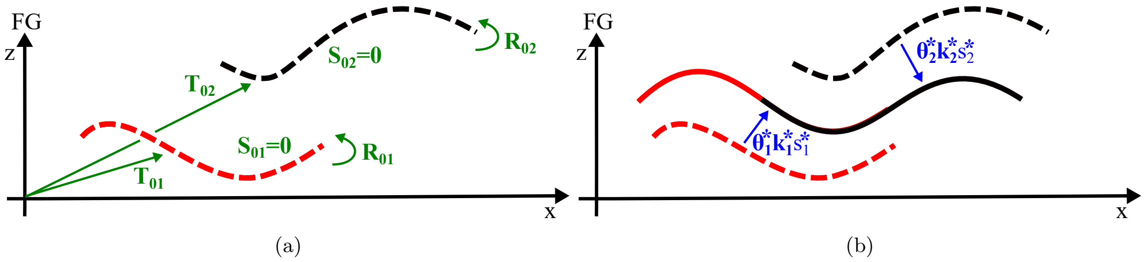

Figure 2: Registration of the segments to reconstruct the entire wavefront. Transformation of the segments into FG using the positioning data of the MAPS (a). Fine registration of the segments using registration algorithms (b).

sum over all overlapping segment pairs, i.e.

$$M_g(\boldsymbol{A}) = \sum_{i,k} M_{ik}(\mathbf{a}_i, \mathbf{a}_k), \tag{1}$$

where M_{ik} denotes a metric for the overlap mismatch between segment i and k. In the PR algorithm[5] M_g is minimized using a Quasi-Newton method which is a well establish method for solving nonlinear optimization problems.[12] In the FPR algorithm $M_g(\boldsymbol{A})$ is approximated by a quadratic function which can be efficiently minimized. The approximation is achieved by linearizing the transformation of a segment with respect to the corresponding parameters $\boldsymbol{a}_i$.[6] The minimization of the quadratic function is then carried out by solving a matrix equation

$$\boldsymbol{Q}^T \boldsymbol{Q} \boldsymbol{A} = \boldsymbol{Q}^T \boldsymbol{B}, \tag{2}$$

with $\boldsymbol{Q} \in \mathbb{R}^{V \times 7U}$ and $\boldsymbol{B} \in \mathbb{R}^V$ where V denotes the total number of sampling points that contribute to Eq. 1. Equation 2 is in particular solved using a Cholesky decomposition.[13] As the approximation is only valid for sufficiently small parameters, the FPR algorithm yields significantly larger registration errors in cases of large uncertainties in the MAPS. This issue is tackled in the IFPR algorithm where M_g is minimized in an iterative manner.[7] Starting from $\boldsymbol{T}_{0i}$, $\boldsymbol{R}_{0i}$ and S_{0i}, the transformation of the segments into FG is corrected in each iteration towards the minimum of M_g. In an iteration m the metric for the global overlap mismatch between the segments that are transformed by the previously corrected transformation, i.e. $\boldsymbol{T}_{m-1i}$, $\boldsymbol{R}_{m-1i}$ and S_{m-1i}, is approximated by a quadratic function. The approximated metric is then efficiently minimized, leading to a further correction of the transformation into FG given by

$$\begin{aligned} \mathbf{T}_{mi} &= \mathbf{R}_{m-1i}\, \boldsymbol{k}_i^* + \mathbf{T}_{m-1i} \\ \mathbf{R}_{mi} &= \mathbf{R}_{m-1i}\, \Re(\boldsymbol{\theta}_i^*) \\ S_{mi} &= S_{m-1i} + s_i^*. \end{aligned} \tag{3}$$

The iteration is stopped when the relative decrease of M_g is smaller than a specific threshold indicating that the transformation for the minimization of the metric is obtained.

3. EXPERIMENTAL RESULTS

Using the measurement system illustrated in Fig. 1, a plane and a divergent wavefront are measured.
The *plane wavefront* is generated by a meniscus lens (LE1015-A, Thorlabs, USA) which is illuminated using a single mode fiber positioned at a distance of 200 mm (focal length) from the lens. The plane wavefront has a diameter of 46 mm and is measured in 69 segments. Each segment is measured using a square sensor aperture with a side length of 6.9 mm. This leads to 2800 lenslets used for the measurement of a segment where the size of a lenslet is equal to $130 \times 130\,\mu m^2$. The average overlap area between the measurements is 30 % of the area of the sensor aperture (47.6 mm^2). The segments are reconstructed using a spline-based zonal reconstruction

algorithm.[14] Using the positioning data of the MAPS to register the segments, leads to an RMS overlap mismatch of $6\,\mu m$ between the segments. The ICP, PR, FPR and IFPR algorithm, are used to obtain a fine registration of the segments and the results are illustrated in Fig. 3. The results show, in particular, the difference (e_{tot}) between the reconstructed wavefront and a plane (nominal wavefront) which is fitted into the reconstructed wavefront in the least squares sense. The difference is equal to the sum of the wavefront aberration and the registration error, i.e.

$$e_{tot} = e_{ab} + e_{reg}, \tag{4}$$

where the latter one depends on the type of the registration algorithm leading to different results. Besides the PV and RMS value of the difference, the RMS overlap mismatch between the segments after the registration is determined to enable an assessment of the registration performance.
In addition to the wavefront aberration and the registration error, there are measurement noise and systematic measurement errors. Typically, these errors are small, however, if the measurement noise is smaller than the systematic measurement errors, too large in-plane shifts of the segments might be the result of the fine registration. To solve this problem, artificial white noise with a standard deviation of $30\,nm$ and a zero mean value is added via software to the segments. After the registration, the artificial noise is removed from each segment.
The ICP algorithm reconstructs the plane wavefront with a gap indicating large in-plane shifts of the segments. This can be explained by the fact that the ICP algorithm registers the segments sequentially, where the segments are one-by-one registered with the reconstructed wavefront, leading to a stronger accumulation of registration errors. Local minima in Eq. 1 cause the PR algorithm to stop the registration at an RMS overlap mismatch of $180\,nm$. This results in a wavefront with an RMS difference of $3\,\mu m$ significantly deviating from the results of the other algorithms. The IFPR and FPR algorithm attain high-quality registration results with an RMS overlap mismatch of $14\,nm$ and $17\,nm$, respectively. As the FPR algorithm corresponds to the IFPR algorithm with one iteration, the IFPR algorithm needs 2 iterations to obtain the result where in the second iteration only a small decrease of the RMS overlap mismatch of $3\,nm$ is attained.

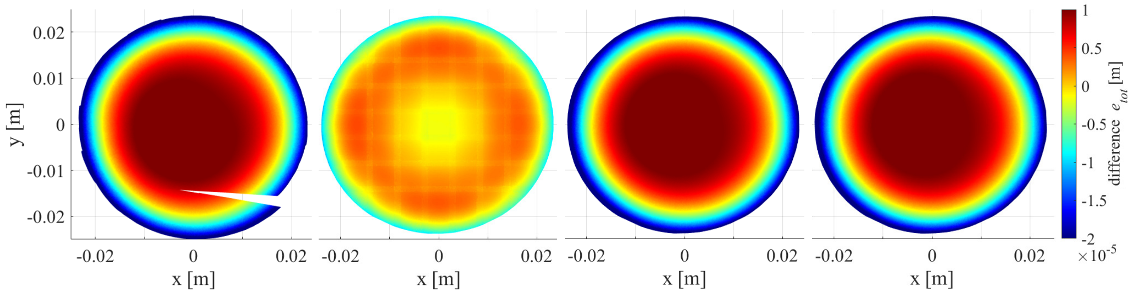

(a) ICP
RMS = $10\,\mu m$
PV = $37.8\,\mu m$
RMS OM = $20\,nm$

(b) PR
RMS = $3\,\mu m$
PV = $15\,\mu m$
RMS OM = $180\,nm$

(c) FPR
RMS = $10\,\mu m$
PV = $36.9\,\mu m$
RMS OM = $17\,nm$

(d) IFPR
RMS = $10\,\mu m$
PV = $37\,\mu m$
RMS OM = $14\,nm$

Figure 3: Plane wavefront. A plane is fitted into the reconstructed plane wavefront and the difference between the reconstructed wavefront and the plane is illustrated for the ICP (a), PR (b), FPR (c) and IFPR (d) algorithm. The RMS and the PV of the difference are determined along with the RMS overlap mismatch (OM) between the registered segments.

The *divergent wavefront* is generated by a microscope objective (Olympus DPlan 40 0.65 160/0.17, Olympus, Japan) which is illuminated with a collimated beam (see Fig. 1). The wavefront has a divergence of 81° and is measured at a radius of $25\,mm$. The wavefront is measured in 67 segments, where each segment is measured using a circular sensor aperture with a radius of $3.45\,mm$, leading to 2200 lenslets per segment. The average overlap area between the measurements is 30 % of the area of the sensor aperture ($37.4\,mm^2$). The segments are reconstructed with the same zonal reconstruction algorithm as for the plane wavefront.
The RMS overlap mismatch between the segments is $30\,\mu m$ if the positioning data of the MAPS is used to

Pre-Print version of the article: Nikolaus Berlakovich, Martin Fuerst, Ernst Csencsics, and Georg Schitter, "Reconstruction of optical wavefronts with parallel registration algorithms," *SPIE Optics + Photonics 2022* Vol. 12221, pp. 192–198, 2022. DOI: 10.1117/12.2632961

register the segments. Analogous to the registration of the plane wavefront, artificial white noise with a standard deviation of $40\,nm$ and a zero mean value is added via software to the segments to prevent the segments from too large in-plane shifts during fine registration. After the application of the registration algorithms, the artificial noise is removed from the segments. The nominal wavefront (sphere) is fitted into the reconstructed wavefront and the difference between nominal and reconstructed wavefront is illustrated in Fig. 4 for the ICP, PR, FPR and IFPR algorithm. The ICP algorithm registers the divergent segments with huge gaps and a large RMS overlap mismatch. Reasons for the bad result of the ICP algorithm are first, the sequential approach for the registration, and second, the fact that the algorithm does not consider wavefront propagation which becomes relevant for the reconstruction of divergent or freeform wavefronts. Dust and scratches on the lenses in the microscope objective result in an occlusion of the wavefront at some locations, where the SHS measures either nothing or strong and high-frequency dynamics of the wavefront. The registration of segments at these locations is a challenge. First, the segments might not have the same shape in the overlap area which is essential for the registration algorithm. Second, the high-frequency dynamics lead to local minima in the overlap mismatch for small in-plane shifts of the segments in which the registration algorithm might get stuck. The result of the PR algorithm shows an RMS overlap mismatch of $467\,nm$. The IFPR algorithm attains in total an RMS overlap mismatch of $173\,nm$, where the RMS overlap mismatch significantly decreases to $68\,nm$ if the parts of the wavefront with the high-frequency dynamics (circled in red in Fig. 4d) are omitted. As expected, the reconstructed wavefront is similar to a sphere with an RMS difference equal to $390\,nm$ and $178\,nm$ if the parts with the high-frequency dynamics are neglected. The IFPR algorithm needs 9 iterations to register the divergent segments indicating that the approximation in the FPR algorithm is not sufficient to attain the desired reduction of the overlap mismatch. The RMS overlap mismatch of the FPR algorithm equals $1000\,nm$ and $276\,nm$ if the high-frequency dynamics are neglected. The approximation of the high-frequency dynamics is of high quality only for small registering parameters, however, large registering parameters are necessary to compensate for the initial overlap mismatch with an RMS value of $30\,\mu m$ resulting in an increased residual overlap mismatch in the result of the FPR algorithm.

The algorithms are implemented on a personal computer with $2.6\,GHz$. Except for the IFPR algorithm, each registration algorithm needs for the reconstruction of both wavefronts computation times at the same order of magnitude as depicted in Table 1. The IFPR algorithm needs a significantly larger computation time for the divergent wavefront, as 9 iterations are necessary to reconstruct the divergent wavefront while only 2 iterations are necessary to reconstruct the plane wavefront.

In summary, the superiority of a parallel registration algorithm as compared to a sequential registration algorithm is shown, as the parallel registration algorithms are able to reconstruct the plane and the divergent wavefront without gaps. Especially the IFPR algorithm attains a small RMS overlap mismatch between the segments down to a few tens of nanometers which is for the divergent wavefront a factor of 10 smaller than the RMS overlap mismatch attained by the ICP algorithm.

Table 1: **Computation time of the ICP, PR, FPR and IFPR algorithm for the reconstruction of the plane and the divergent wavefront. The algorithms run on a personal computer ($2.6\,GHz$).**

	ICP	PR	FPR	IFPR
plane (s)	3.7	680	0.2	0.37
divergent (s)	8.5	1000	0.3	2

4. CONCLUSION

In this paper, an experimental evaluation of parallel registration algorithms, in particular, the PR,[5] the FPR[6] and the IFPR[7] algorithm is presented. The evaluation is based on two use cases, i.e. the reconstruction of a plane and a divergent wavefront generated by a meniscus lens and a microscope objective, respectively. In the scope of the evaluation, the well-known ICP algorithm is considered as a benchmark. The ICP algorithm reconstructs both wavefronts with at least one gap. A reason for this is that the ICP algorithm registers the segments sequentially while the other algorithms register the segments in parallel, where the accumulation of registration errors is typically reduced. The PR algorithm attains moderate results which can be explained by the fact that the PR algorithm is more prone to get stuck in local minimal than the IFPR and FPR algorithm. The FPR algorithm shows a good registration performance with respect to the plane wavefront where an RMS

Pre-Print version of the article: Nikolaus Berlakovich, Martin Fuerst, Ernst Csencsics, and Georg Schitter, "Reconstruction of optical wavefronts with parallel registration algorithms," *SPIE Optics + Photonics 2022* Vol. 12221, pp. 192–198, 2022. DOI: 10.1117/12.2632961

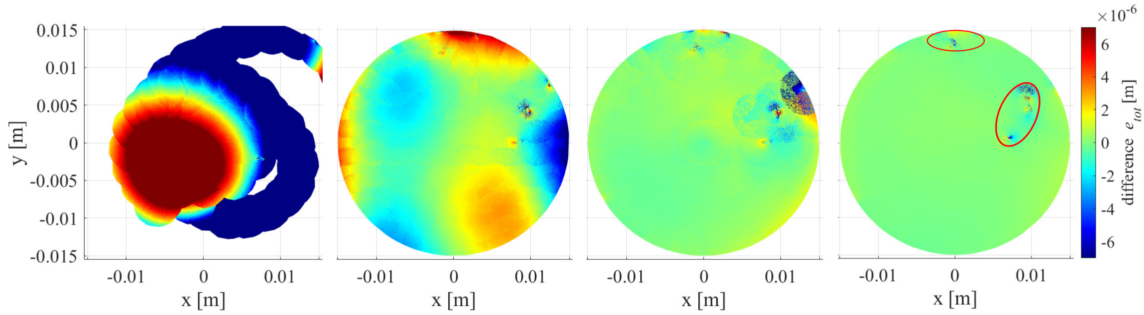

(a) ICP
RMS = 19 μm
PV = 161 μm
RMS OM = 1400 nm

(b) PR
RMS = 1.9 μm
PV = 34 μm
RMS OM = 467 nm
RMS OM$_{red}$ = 420 nm

(c) FPR
RMS = 0.88 μm
PV = 32 μm
RMS OM = 1000 nm
RMS OM$_{red}$ = 276 nm

(d) IFPR
RMS = 0.39 μm
PV = 26 μm
RMS OM = 173 nm
RMS OM$_{red}$ = 68 nm

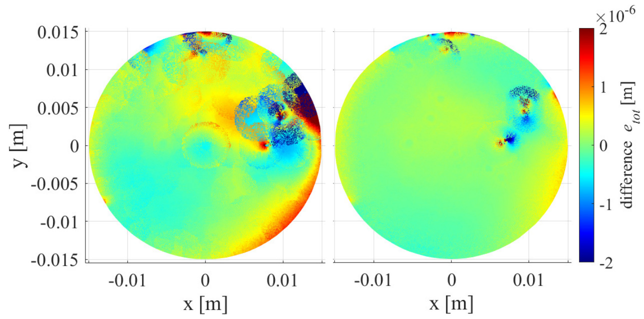

(e) FPR

(f) IFPR

Figure 4: Divergent wavefront. A sphere is fitted into the reconstructed divergent wavefront and the difference between the reconstructed wavefront and the sphere is illustrated for the ICP (a), PR (b), FPR (c,e) and IFPR (d,f) algorithm. (e) and (f) show the same results as (c) and (d), respectively, at a different scale. The RMS and the PV of the difference are determined along with the RMS overlap mismatch (OM) between the registered segments.

overlap mismatch between the segments of 17 nm is attained. The IFPR algorithm attains the smallest RMS overlap mismatch with 14 nm for the plane wavefront and 173 nm for the divergent wavefront. The RMS overlap mismatch in the divergent wavefront decreases to 68 nm, if parts of the wavefront are omitted that include high-frequency dynamics due to occlusions in the microscope objective.

ACKNOWLEDGMENTS

The financial support by the Christian Doppler Research Association, the Austrian Federal Ministry for Digital and Economic Affairs, and the National Foundation for Research, Technology and Development, as well as Micro-Epsilon Messtechnik GmbH & Co. KG and Micro-Epsilon Atensor GmbH is gratefully acknowledged.

REFERENCES

[1] Tyson, R. K., [*Adaptive optics engineering handbook*], Marcel Dekker New York (2000).
[2] Rocktäschel, M. and Tiziani, H., "Limitations of the shack–hartmann sensor for testing optical aspherics," *Optics & Laser Technology* **34**(8), 631–637 (2002).
[3] Fuerst, M. E. and Schitter, G., "Scanning wavefront sensor for measurement of highly divergent wavefronts," *IFAC-PapersOnLine* **52**(15), 25–30 (2019).

[4] Fuerst, M. E., Csencsics, E., Berlakovich, N., and Schitter, G., "Automated measurement of highly divergent optical wavefronts with a scanning shack–hartmann sensor," *IEEE Transactions on Instrumentation and Measurement* **70**, 1–9 (2020).

[5] Berlakovich, N., Fuerst, M. E., Csencsics, E., and Schitter, G., "Robust wavefront segment registration based on a parallel approach," *Applied Optics* **60**(6), 1578–1586 (2021).

[6] Berlakovich, N., Csencsics, E., Fuerst, M., and Schitter, G., "Fast, precise, and shape-flexible registration of wavefronts," *Applied Optics* **60**(23), 6781–6790 (2021).

[7] Berlakovich, N., Csencsics, E., Fuerst, M., and Schitter, G., "Iterative parallel registration of strongly misaligned wavefront segments," *Optics Express* **29**(21), 33281–33296 (2021).

[8] Chen, Y. and Medioni, G., "Object modelling by registration of multiple range images," *Image and vision computing* **10**(3), 145–155 (1992).

[9] Sheldakova, J., Kudryashov, A., Zavalova, V., and Romanov, P., "Shack-hartmann wavefront sensor versus fizeau interferometer for laser beam measurements," in [*Laser Resonators and Beam Control XI*], **7194**, 71940B, International Society for Optics and Photonics (2009).

[10] Neal, D. R., Copland, J., and Neal, D. A., "Shack-hartmann wavefront sensor precision and accuracy," in [*Advanced Characterization Techniques for Optical, Semiconductor, and Data Storage Components*], **4779**, 148–160, International Society for Optics and Photonics (2002).

[11] Huang, L., Xue, J., Gao, B., Zuo, C., and Idir, M., "Zonal wavefront reconstruction in quadrilateral geometry for phase measuring deflectometry," *Applied optics* **56**(18), 5139–5144 (2017).

[12] Gill, P. E., Murray, W., and Wright, M. H., [*Practical optimization*], SIAM (2019).

[13] Trefethen, L. N. and Bau III, D., [*Numerical linear algebra*], vol. 50, Siam (1997).

[14] Huang, L., Xue, J., Gao, B., Zuo, C., and Idir, M., "Spline based least squares integration for two-dimensional shape or wavefront reconstruction," *Optics and Lasers in Engineering* **91**, 221–226 (2017).

Pre-Print version of the article: Nikolaus Berlakovich, Martin Fuerst, Ernst Csencsics, and Georg Schitter, "Reconstruction of optical wavefronts with parallel registration algorithms," *SPIE Optics + Photonics 2022* Vol. 12221, pp. 192–198, 2022.
DOI: 10.1117/12.2632961